Rabi resonance in frequency conversion by four-wave mixing in lasers and its connection with the multimode laser instability

F. Castelli, L. A. Lugiato, and R. Pirovano
Dipartimento di Fisica, via Celoria 16, 20133 Milano, Italy
(Received 16 November 1993)

We analyze the behavior of a laser upon injection of a weak-field resonant with a cavity mode adjacent to the lasing mode; the four-wave-mixing coupling generates also a field with the frequency of the symmetrical adjacent mode. Using the Maxwell-Bloch equations, we show that under appropriate conditions there is a spectacular amount of frequency conversion, with a peak when the free spectral range is equal to the Rabi frequency of the laser field multiplied by $\sqrt{2}$. The origin of this effect is identified with the help of the linear stability analysis of the free-running laser, which shows also the deep connections with the classical laser instability, predicted by Risken and Nummedal [J. Appl. Phys. **39**, 4662 (1968)] and Graham and Haken [Z. Phys. **213**, 420 (1968)]. The Rabi peak is a precursor of the multimode laser instability, but it arises for smaller values of the pump parameter and is only weakly sensitive to the transverse shape of the laser beam.

PACS number(s): 42.65.Hw, 42.65.Ky

I. INTRODUCTION

Some recent papers [1] analyze the possibility of obtaining frequency conversion in diode lasers by injecting into the laser cavity a coherent field of frequency ω_1 detuned from the laser frequency ω_0. The injected beam is weak enough in order to avoid injection locking, and the mechanism of four-wave mixing generates another field of frequency $\omega_{-1}=2\omega_0-\omega_1$ symmetrically located with respect to the laser frequency. By following this procedure one can obtain a frequency conversion $|\omega_1-\omega_{-1}|/2\pi$ on the order of 100 GHz, for example, which is interesting for practical applications.

Loudon and collaborators [2] studied this mechanism both theoretically and experimentally, considering the case of a single-mode laser and of an injected signal with a frequency offset $\omega_1-\omega_0$ on the order of the cavity linewidth k. In the theoretical investigations that we present here, we consider instead a multimode regime, in which ω_0 and ω_1 correspond to two different frequencies of the laser cavity; this configuration allows for a larger frequency conversion, because the frequency offset $\omega_1-\omega_0$ is now equal to the free spectral range of the cavity. In our analysis, we use the classic Maxwell-Bloch equations for the laser field interacting with a homogeneously broadened set of two-level atoms [3–6]; this model allows for studying also the possible effects which arise from atomic coherence, which is not the case for the rate equations which are standardly used for the description of diode or semiconductor lasers.

The main results of our analysis emerge in the case in which the relaxation rate $\gamma_\perp$ of the atomic polarization (or atomic linewidth) is much larger than the damping rate $\gamma_\parallel$ of the population inversion; this situation is common in a large class of lasers which includes semiconductor lasers. Precisely, we find that there is a spectacular amount of frequency conversion, in the sense that the ratio of the intensity of the converted field (with frequency ω_{-1}) and that of the injected signal can be much larger than unity; the output intensities of both fields with frequencies ω_1 and ω_{-1} display a peak when the frequency offset $\omega_1-\omega_0$ is equal to the Rabi frequency of the laser field (multiplied by $\sqrt{2}$).

At first sight, the existence of a Rabi resonance in the signal field may appear not surprising, because it is well known that a weak probe beam which interacts with a two-level medium saturated by a detuned strong beam can experience gain [7], and this gain is maximum when the frequency offset between the two beams is equal to the Rabi frequency of the strong field [7–9]. The four-wave-mixing enhancement of the gain is also well known [9]. In our case, however, there is a basic element which is absent in Refs. [7–9] and affects dramatically the behavior of the system; namely, the optical cavity. As a consequence, the gain we calculate is not that of a probe beam, but is defined as the ratio of the output intensity (for each of the two fields with frequency ω_1 and ω_{-1}) to the input intensity *in the stationary state of the system.* The element which best emphasizes the difference between our results and the previous investigations is the surprising feature that our results emerge just in the limit of $\gamma_\parallel/\gamma_\perp \ll 1$, in which the four-wave-mixing coupling between the two side modes becomes small too. As a matter of fact, the mechanisms which originate our effects will be elucidated with the help of the linear stability analysis of the stationary solution of the free-running laser. This analysis was performed 25 years ago by Risken and Nummedal [3] and Graham and Haken [10] and led to the prediction of the multimode instability of the laser [3,10]. Even if this instability has not yet been observed experimentally to our knowledge, it remains a classic result in the field of laser dynamics, and it is in our opinion very interesting that the Rabi resonance predicted in this paper appears intimately related with this instability.

In Sec. II we review the Maxwell-Bloch equations and

their formulation in terms of modal amplitudes for the field and atomic variables. Section III discusses the response of the system upon injection of the external signal, both analytically and with the help of numerical simulations. In Sec. IV we illustrate the connections with the multimode laser instability. All the results shown in Secs. II–IV are obtained in the framework of a plane-wave theory. In Sec. V we consider, instead, the case of an electric field with a Gaussian radial profile, and compare the results with those of the plane-wave theory. The final Sec. VI summarizes and comments upon the main results of the paper.

II. MODEL

We consider the Maxwell-Bloch equations for a ring cavity laser filled by a two-level medium in the plane-wave and paraxial approximation [3–6],

$$\frac{\partial F}{\partial t}+c\frac{\partial F}{\partial z}=-k(F-2CP)\ , \tag{1a}$$

$$\frac{\partial P}{\partial t}=\gamma_{\perp}(FD-P)\ , \tag{1b}$$

$$\frac{\partial D}{\partial t}=-\gamma_{\parallel}[\tfrac{1}{2}(F^{*}P+FP^{*})+D-1]\ , \tag{1c}$$

where the normalized variables $F(z,t)$, $P(z,t)$, and $D(z,t)$ denote the slowly varying envelope of the electric field, the atomic polarization, and the population inversion, respectively. $2C$ is the pump parameter (the laser threshold is $2C=1$), k is the cavity damping constant, or cavity linewidth, which corresponds to one-half the mean lifetime of photons in the cavity; $\gamma_{\perp}$ is the atomic linewidth or transverse relaxation rate, while $\gamma_{\parallel}$ is the longitudinal relaxation rate. The last two parameters arise from spontaneous emission and from other mechanisms of homogeneous broadening.

Equation (1a) must be accompanied by the ring cavity periodic boundary condition [3–5]

$$F(L,t)=F(0,t)\ , \tag{2}$$

where L is the cavity length. In writing Eqs. (1) we assumed that the atomic line is exactly resonant with one of the longitudinal modes of the cavity, whose frequency is taken as the reference frequency of the electric field.

We can expand the variables F,P,D on the basis of the longitudinal modes of the cavity [4,5]:

$$F(z,t)=\sum_{n=-\infty}^{+\infty}\exp\left[-in\alpha\left[t-\frac{z}{c}\right]\right]f_n(t)\ , \tag{3a}$$

$$P(z,t)=\sum_{n=-\infty}^{+\infty}\exp\left[-in\alpha\left[t-\frac{z}{c}\right]\right]p_n(t)\ , \tag{3b}$$

$$D(z,t)=\sum_{n=-\infty}^{+\infty}\exp\left[-in\alpha\left[t-\frac{z}{c}\right]\right]d_n(t)\ , \tag{3c}$$

where α is the free spectral range

$$\alpha=\frac{2\pi c}{L}\ .$$

The choice of the orthonormal basis functions $\exp(in\alpha z/c)$ satisfies condition (2). By substituting the modal decomposition (3) into Eqs. (1), one obtains an infinite set of coupled ordinary differential equations for the mode amplitudes $f_n,f_n^{*},p_n,p_n^{*},d_n$. Their explicit form is given by [4,5]

$$\dot{f}_n=-k(f_n-2Cp_n)\ , \tag{4a}$$

$$\dot{p}_n=\gamma_{\perp}\left[\sum_{n'}f_{n'}d_{n-n'}-\left[1-i\frac{n\alpha}{\gamma_{\perp}}\right]p_n\right]\ , \tag{4b}$$

$$\dot{d}_n=-\gamma_{\parallel}\left[\tfrac{1}{2}\sum_{n'}(f^{*}_{-n'}p_{n-n'}+f_{n'}p^{*}_{n'-n})+d_n\left[1-i\frac{n\alpha}{\gamma_{\parallel}}\right]-\delta_{n,0}\right]\ . \tag{4c}$$

The equations for f_n^{*} and p_n^{*} are the complex conjugate of Eqs. (4a) and (4b), respectively, while $d_n^{*}=d_{-n}$.

The set of Eqs. (4) admits an infinite number of exact single-mode stationary intensity solutions [4]. The one in which only the mode $n=0$, exactly resonant with the atomic line, is excited has the lowest threshold. It can be calculated by putting $\dot{f}_n=\dot{f}_n^{*}=\dot{p}_n=\dot{p}_n^{*}=\dot{d}_n=0$ with the result

$$\begin{aligned}|f_n^{S}|&=(2C-1)^{1/2}\delta_{n,0}\ ,\\ p_n^{S}&=\frac{f_0^{S}}{1+|f_0^{S}|^2}\delta_{n,0}\ ,\\ d_n^{S}&=\frac{1}{1+|f_0^{S}|^2}\delta_{n,0}\ ,\end{aligned} \tag{5}$$

where the superscript S indicates the stationary values. The phase on f_n^{S} is completely arbitrary.

III. ANALYTICAL AND NUMERICAL RESULTS (PLANE-WAVE THEORY)

Next, we inject into the laser a signal ε whose frequency is equal to that of the sidemode $n=1$, so that Eq. (4a) becomes

$$\dot{f}_n=-k[f_n-\varepsilon\delta_{n,1}-2Cp_n]\ . \tag{4a'}$$

When the signal intensity ε^2 is large enough the laser locks to the signal frequency and the system approaches a new stationary intensity solution in which only the mode $n=1$ is excited. In this paper, however, we focus on the case of a weak signal intensity ε^2 which cannot produce injection locking.

As a consequence of the four-wave-mixing (4WM) process involving the three modes $n=0$, $n=1$, and $n=-1$, the system will build up also the symmetrical side mode $n=-1$. The problem is to find the steady-state amplitude of the mode $n=-1$, and to compare it with the amplitude of the input field, in order to assess how much frequency conversion from mode $n=1$ to mode $n=-1$ is obtained. The calculation can be performed analytically in the limit of the weak signal by setting

$$f_n = f_n^S + \varepsilon f_n^{(1)} + o(\varepsilon^2) ,$$
$$p_n = p_n^S + \varepsilon p_n^{(1)} + o(\varepsilon^2) , \quad (6)$$
$$d_n = d_n^S + \varepsilon d_n^{(1)} + o(\varepsilon^2) ,$$

and by inserting Eqs. (6) into Eqs. (4a'), (4b), and (4c), and into the complex conjugates of Eqs. (4a') and (4b). Neglecting all terms proportional to ε^2, one obtains an infinite set of differential equations for $f_n^{(1)}, f_n^{(1)*}, p_n^{(1)}, p_n^{(1)*}, d_n^{(1)}$. This system of equations decouples, giving rise to a set of five linear differential equations for every fixed value of n; the coupled variables are $f_n^{(1)}, f_{-n}^{(1)*}, p_n^{(1)}, p_{-n}^{(1)*}, d_n^{(1)}$. The arbitrary phase of f_0^S does not affect at all the results, and can be taken equal to zero.

We solve these equations at steady state (by setting time derivatives equal to zero) and obtain the following expressions for the stationary values of the output signals $f_1^{(1)}$ and $f_{-1}^{(1)}$:

$$f_1^{(1)} = [\tilde{\alpha}\sqrt{\tilde{\gamma}}(3|f_0^S|^2 - 2\tilde{\alpha}^2 + 2) + 2i(|f_0^S|^2 - \tilde{\alpha}^2\tilde{\gamma} - \tilde{\alpha}^2)][\mathcal{D}(C,\tilde{\alpha},\tilde{\gamma})]^{-1} , \quad (7a)$$

$$f_{-1}^{(1)} = [|f_0^S|^2(-\tilde{\alpha}\sqrt{\tilde{\gamma}} + 2i)][\mathcal{D}^*(C,\tilde{\alpha},\tilde{\gamma})]^{-1} , \quad (7b)$$

with

$$\mathcal{D}(C,\tilde{\alpha},\tilde{\gamma}) = 2\tilde{\alpha}\sqrt{\tilde{\gamma}}(2|f_0^S|^2 - \tilde{\alpha}^2 - i\tilde{\alpha}\sqrt{\tilde{\gamma}}) , \quad (8a)$$

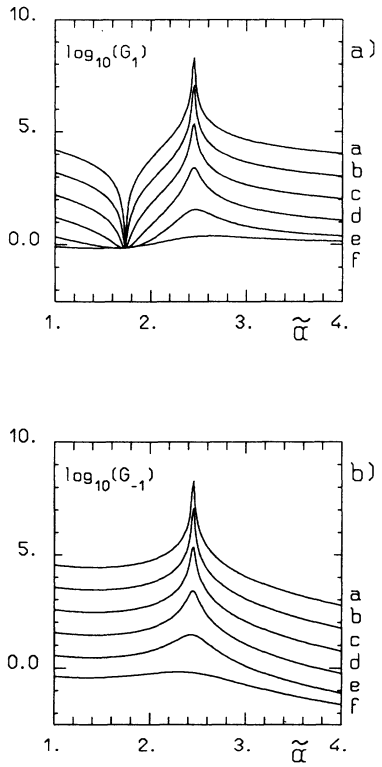

FIG. 1. (a) The pump parameter is $C=2$. The gain $G_1 = |f_1|^2/\varepsilon^2$ of the signal field is graphed (in logarithmic scale) as a function of $\tilde{\alpha}$ for several values of $\tilde{\gamma}$: (a) $\tilde{\gamma}=10^{-5}$, (b) $\tilde{\gamma}=10^{-4}$, (c) $\tilde{\gamma}=10^{-3}$, (d) $\tilde{\gamma}=10^{-2}$, (e) $\tilde{\gamma}=10^{-1}$, (f) $\tilde{\gamma}=1$. (b) Same as in (a), but for the gain G_{-1} of the frequency-converted field f_{-1}.

$$\tilde{\gamma} = \gamma_\parallel/\gamma_\perp , \quad \tilde{\alpha} = \alpha/(\gamma_\perp\gamma_\parallel)^{1/2} , \quad (8b)$$

while the first-order corrections to f_n^S with $n \neq 1, -1$ turn out to be equal to zero.

Equations (7) and (8) allow us to analyze the weak signal regime in which the cavity mode with $n=0$ and the two adjacent modes coexist. Their intensities $|f_1|^2$ and $|f_{-1}|^2$ depend on three parameters: the pump parameter $2C$, and the ratios $\tilde{\gamma}$ and $\tilde{\alpha}$. Figures 1(a) and 1(b) show the gains of the two fields,

$$G_1 = \frac{|f_1|^2}{\varepsilon^2} , \quad G_{-1} = \frac{|f_{-1}|^2}{\varepsilon^2} , \quad (9)$$

where f_i $(i=1,-1)$ are the amplitudes of the two adjacent modes (f_1 corresponds to the mode which is excited by the injected signal ε, f_{-1} to the mode which grows up by 4WM frequency conversion) as a function of $\tilde{\alpha}$ for $C=2$ (four times above threshold) and for several values of $\tilde{\gamma}$. The figures show some predominant features, which emerge when $\tilde{\gamma}$ becomes small.

(i) The system develops a remarkable susceptibility with respect to the injection of the signal. Such a sensitivity, which affects both fields $f_{\pm 1}$, turns out to be advantageous for the frequency conversion; for example, when $\tilde{\alpha}=3$ and $\tilde{\gamma}=10^{-4}$, G_{-1} is larger than 10^3.

(ii) There is a noteworthy peak in both gains for

$$\tilde{\alpha} = \sqrt{2}|f_0^S| = \{2(2C-1)\}^{1/2} , \quad (10a)$$

i.e., taking Eq. (8b) into account,

$$\alpha = \sqrt{2}\Omega_R , \quad \Omega_R = |f_0^S|\sqrt{\gamma_\perp\gamma_\parallel} , \quad (10b)$$

where Ω_R is the Rabi frequency of the field in the single-mode stationary state of the laser in absence of the injected signal. This is a consequence of the fact that the real part of the function $\mathcal{D}$ (Eq. 8) is equal to zero when $\tilde{\alpha}=\sqrt{2}|f_0^S|$, while the imaginary part is proportional to $\tilde{\gamma}$.

(iii) The gain G_1 shows a dip when the intermode spacing α is equal to the Rabi frequency Ω_R, in fact, the numerator of Eq. (7a) approaches to zero for $\alpha=\Omega_R$ in the limit $\tilde{\gamma}\to 0$.

(iv) The peak marks an exchange between the two fields f_1 and f_{-1}: on the right (on the left) of the peak $|f_1|$ ($|f_{-1}|$) is larger than $|f_{-1}|$ ($|f_1|$). The dependence

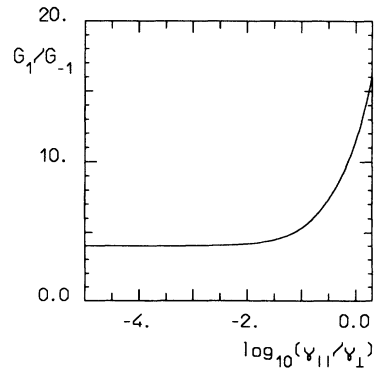

FIG. 2. The ratio of G_1 to G_{-1} is shown as a function of $\log_{10}(\tilde{\gamma})$, for $\tilde{\alpha}=3$ and $C=2$.

of the ratio G_1/G_{-1} on $\tilde{\gamma}$ is illustrated in Fig. 2; it turns out to be nearly constant for a wide range of values of $\tilde{\gamma}$.

We can see from Figs. 1(a) and 1(b) that the peak tends to vanish when $\tilde{\gamma}$ becomes of order of unity; on the other hand, as $\tilde{\gamma}$ decreases, the amplitudes $|f_1|$ and $|f_{-1}|$ for every value of $\tilde{\alpha}$ become larger and larger and the peak is narrower and narrower. As a matter of fact, one can verify from Eqs. (7) and (8) that the fields f_1 and f_{-1} scale as $1/\sqrt{\tilde{\gamma}}$ when $\tilde{\gamma}$ is small.

A very important point is that the previous results are completely independent of the cavity damping constant k. On the other hand, the condition $\tilde{\gamma} \ll 1$ is met quite often in lasers; for example, in class-B lasers ($\gamma_\perp \gg k \gg \gamma_\parallel$). If we consider, for instance, the values $\gamma_\perp = 10^{13}$ rad/s and $\gamma_\parallel = 10^9$ rad/s, which are compatible with the case of semiconductor lasers, the value $\tilde{\alpha}=3$ considered above at point 1 corresponds to a frequency conversion (from mode 1 to mode -1) of ~ 100 GHz.

The results of the previous perturbative analysis have been compared with those obtained by numerical integration of Eqs. (4a'), (4b), and (4c). For definiteness, we assumed that $\gamma_\perp \gg k, \gamma_\parallel$, a condition which allows us to eliminate adiabatically the polarization variables by setting $\dot{p}_n = 0$ in Eq. (4b). In our numerical calculations we considered only the five modes $n = 0, \pm 1, \pm 2$, and used the values $\gamma_\perp = 10^{13}$ rad/s, $\gamma_\parallel = 10^9$ rad/s, $k = 3 \times 10^{10}$ rad/s (again, compatible with semiconductor lasers) and selected the pump parameter value $C = 2$. After a transient, the system reaches a stationary state [11] with three excited modes f_0, f_1, and f_{-1}, while the amplitudes for the modes $n = \pm 2$ turn out to be negligible. The stationary values for the amplitudes f_0, f_1, and f_{-1} basically coincide with those calculated with the perturbative analysis, except in a region of width ~ 50 GHz around the point $\alpha = \sqrt{2}\Omega_R$, where the linearization introduced by Eqs. (6) fails. Figure 3 shows the steady-state values of G_i ($i = 0, \pm 1$) (where G_0 is defined as $|f_0|^2/\varepsilon^2$) as a function of $\tilde{\alpha}$. As one can see, the numerical integration confirms the existence of a peak (much reduced in comparison with the prediction of the linearized analysis) for the amplitudes f_1 and f_{-1} when $\alpha = \sqrt{2}\Omega_R$; in correspondence of this peak the amplitude f_0 shows a dip, whereas in the linearized analysis f_0 remains unperturbed. Also, the existence of a dip for G_1 at $\alpha = \Omega_R$ is confirmed by the numerical simulation.

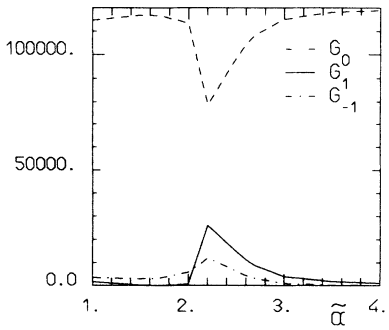

FIG. 3. The numerical steady-state values of G_0, G_1, and G_{-1} are shown as a function of $\tilde{\alpha}$, for $\gamma_\perp = 10^{13}$ rad/s, $\gamma_\parallel = 10^9$ rad/s, $k = 3 \times 10^{10}$ rad/s, and $C = 2$.

IV. CONNECTION WITH THE MULTIMODE LASER INSTABILITY

The characteristic properties 1 and 2 described in the previous section can be understood by considering that the small signal problem amounts to the set of modal equations linearized around the single-mode stationary state of the laser, with the input signal playing the role of an inhomogeneous term in the otherwise homogeneous set of equations. Therefore, the dynamics is governed by the eigenvalues of the homogeneous linearized problem; there are three eigenvalues related to the amplitude fluctuations and two eigenvalues related to phase fluctuations [4].

It turns out that the denominator of Eqs. (7a) and (7b) can be written as [4,12]

$$\mathcal{D} = 2\frac{\lambda_A}{k}\frac{\lambda_P}{k}\left[|f_0^S|^2 + (1 - i\tilde{\alpha}\sqrt{\tilde{\gamma}})\left[1 - i\frac{\tilde{\alpha}}{\sqrt{\tilde{\gamma}}}\right]\right] \times [i + \tilde{\alpha}\sqrt{\tilde{\gamma}}] , \tag{11}$$

where

$$\lambda_A = -k\left[1 - \frac{(1 - |f_0^S|^2) - i\tilde{\alpha}/\sqrt{\tilde{\gamma}}}{(1 - i\tilde{\alpha})(1 - i\tilde{\alpha}/\sqrt{\tilde{\gamma}}) + |f_0^S|^2}\right] , \tag{12a}$$

$$\lambda_P = -k\frac{\tilde{\alpha}\sqrt{\tilde{\gamma}}}{i + \tilde{\alpha}\sqrt{\tilde{\gamma}}} . \tag{12b}$$

(a) λ_P is the phase eigenvalue which is relevant for the long-time evolution in the limit $k \ll \gamma_\perp, \gamma_\parallel$. Evidently, when $\tilde{\gamma}$ becomes small λ_P is small too, i.e., the phase of the modes $1, -1$ evolves very slowly. As usual, in the presence of a slowing down, the system becomes very sensitive to external perturbations. This feature explains the large values of the gains G_1 and G_{-1} for $\tilde{\gamma} \ll 1$.

(b) λ_A is the amplitude eigenvalue which, for $k \ll \gamma_\perp, \gamma_\parallel$, determines the well known multimode laser instability predicted by Risken and Nummedal [3], and Graham and Haken [10]. When $\gamma_\perp$ is also much larger than $\gamma_\parallel$ and $C \gg 1$, this instability appears when $\Omega_R < \alpha < \sqrt{2}\Omega_R$; for $\alpha = \Omega_R$ and $\alpha = \sqrt{2}\Omega_R$, one has it that $\mathrm{Re}(\lambda_A) = 0$.

It is clear that the peak in Figs. 1(a) and 1(b) arises when the modulus of the denominator $\mathcal{D}$ becomes very small; as one can verify, for $\tilde{\gamma} \ll 1$ this condition is reached in correspondence to the upper boundary of the multimode laser instability domain. On the other hand, at the lower boundary $\alpha = \Omega_R$, $|\mathcal{D}|$ is not small and therefore there is no peak; however, curiously enough, this is just the value of α in correspondence to which the gain G_1 displays a dip [Fig. 1(a)].

These considerations illustrate the relations which link our Rabi resonance with the multimode laser instability [3,10]. However, we must note also the following two important differences:

(i) The Rabi resonance phenomenon is independent of the value of k but, on the other hand, requires that $\tilde{\gamma}$ is small, a condition which is not necessary for the mul-

timode laser instability, and

(ii) The multimode laser instability requires that the laser is several times above threshold (for $\bar{\gamma} \ll 1$ one must have $2C \geq 9$), whereas the Rabi resonance is sizable also for substantially smaller values of C.

In conclusion, one can say that the Rabi resonance is basically a *precursor* of the multimode laser instability, and can be experimentally observed with less stringent conditions on the pump parameters C.

V. CASE OF A GAUSSIAN BEAM PROFILE

It is known that the multimode laser instability disappears when one considers a laser beam with a Gaussian radial profile [13,14]. For this reason we studied the frequency-conversion phenomenon, also assuming that the field, instead of the plane-wave configuration considered before, has the Gaussian shape

$$\exp(-r^2/w_0^2) ,$$

where r is the radial variable and w_0 is the beam waist. The modal equations (4a')–(4c) of the plane-wave model are modified in the following way [14]:

$$\dot{\tilde{f}}_n = -k\left[\tilde{f}_n - \tilde{\varepsilon}\delta_{n,1} - 2C\int_0^\infty d\bar{r}\, 4\bar{r}e^{-\bar{r}^2}p_n\right] , \tag{13a}$$

$$\frac{\partial p_n}{\partial t} = \gamma_\perp\left[\sum_{n'}(\tilde{f}_{n'}d_{n-n'})e^{-\bar{r}^2} - \left[1 - i\frac{n\alpha}{\gamma_\perp}\right]p_n\right] , \tag{13b}$$

$$\frac{\partial d_n}{\partial t} = -\gamma_\parallel\left[\tfrac{1}{2}\sum_{n'}(\tilde{f}^*_{-n'}p_{n-n'} + \tilde{f}_{n'}p^*_{n'-n})e^{-\bar{r}^2} + d_n\left[1 - i\frac{n\alpha}{\gamma_\parallel}\right] - \delta_{n,0}\right] , \tag{13c}$$

with

$$\tilde{f}_n = \left[\frac{2}{\pi}\right]^{1/2}\frac{1}{w_0}f_n ,$$

$$\tilde{\varepsilon} = \left[\frac{2}{\pi}\right]^{1/2}\frac{1}{w_0}\varepsilon ,$$

$$\bar{r} = \frac{r}{w_0} .$$

The quantities p_n and d_n depend now not only on time but also on the radial variable $\bar{r}$. By setting $\dot{\tilde{f}}_n = \dot{\tilde{f}}^*_n = \partial p_n/\partial t = \partial p^*_n/\partial t = \partial d_n/\partial t = 0$ in Eqs. (13) with $\tilde{\varepsilon} = 0$, one obtains the single-mode stationary solution governed by the equations [13,14]

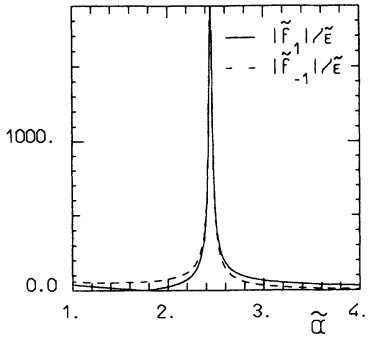

FIG. 4. Case of a Gaussian beam profile. The values of $|\tilde{f}_i|/\tilde{\varepsilon}$ $(i = \pm 1)$ are graphed as a function of $\tilde{\alpha}$ for $C = 2$ and for $\bar{\gamma} = 10^{-4}$.

$$1 - \frac{2C}{|\tilde{f}^S_0|^2}\ln(1+|\tilde{f}^S_0|^2) = 0 ,$$

$$p^S_0 = \frac{\tilde{f}^S_0 e^{-\bar{r}^2}}{1+|\tilde{f}^S_0|^2 e^{-2\bar{r}^2}} , \tag{14}$$

$$d^S_0 = \frac{1}{1+|\tilde{f}^S_0|^2 e^{-2\bar{r}^2}} ,$$

instead of the single-mode plane-wave solution given by Eq. (5).

When the injected signal $\tilde{\varepsilon}$ is different from zero, one obtains, as a consequence of the four-wave mixing process, a stationary regime with the three modes $n = 0, \pm 1$ excited. Performing the linearization with respect to the unperturbed stationary solution for $\tilde{\varepsilon} = 0$, as in the plane-wave case [see Eqs. (6)], one arrives at the following expressions for $\tilde{f}^{(1)}_1$ and $\tilde{f}^{(1)}_{-1}$ at steady state:

$$\tilde{f}^{(1)}_1 = \left\{1 - Ci\frac{\tilde{\alpha}\sqrt{\bar{\gamma}}}{1-i\tilde{\alpha}\sqrt{\bar{\gamma}}}|\tilde{f}^S_0|^2 I(C,\tilde{\alpha},\bar{\gamma}) - 2C\left[1 - i\frac{\tilde{\alpha}}{\sqrt{\bar{\gamma}}}\right]J(C,\tilde{\alpha},\bar{\gamma})\right\}[\mathcal{F}(C,\tilde{\alpha},\bar{\gamma})]^{-1} , \tag{15a}$$

$$\tilde{f}^{(1)}_{-1} = \left[-C\frac{2+i\tilde{\alpha}\sqrt{\bar{\gamma}}}{1+i\tilde{\alpha}\sqrt{\bar{\gamma}}}|\tilde{f}^S_0|^2 I^*(C,\tilde{\alpha},\bar{\gamma})\right][\mathcal{F}^*(C,\tilde{\alpha},\bar{\gamma})]^{-1} , \tag{15b}$$

with

$$\mathcal{F}(C,\tilde{\alpha},\bar{\gamma}) = \left[1 + 2C|\tilde{f}^S_0|^2 I(C,\tilde{\alpha},\bar{\gamma}) - 2C\left[1 - i\frac{\tilde{\alpha}}{\sqrt{\bar{\gamma}}}\right]J(C,\tilde{\alpha},\bar{\gamma})\right] \times \left[1 - 2C\frac{1}{1-i\tilde{\alpha}\sqrt{\bar{\gamma}}}|\tilde{f}^S_0|^2 I(C,\tilde{\alpha},\bar{\gamma}) - 2C\left[1 - i\frac{\tilde{\alpha}}{\sqrt{\bar{\gamma}}}\right]J(C,\tilde{\alpha},\bar{\gamma})\right] \tag{16}$$

and

$$I(C,\tilde{\alpha},\tilde{\gamma})=\int_0^\infty \frac{d\tilde{r}\,4\tilde{r}\,e^{-4\tilde{r}^2}}{[1+|\tilde{f}_0^S|^2e^{-2\tilde{r}^2}]\left[(1-i\tilde{\alpha}\sqrt{\tilde{\gamma}})\left[1-i\frac{\tilde{\alpha}}{\sqrt{\tilde{\gamma}}}\right]+|\tilde{f}_0^S|^2e^{-2\tilde{r}^2}\right]}$$

$$=\frac{1}{\left[(1-i\tilde{\alpha}\sqrt{\tilde{\gamma}})\left[1-i\frac{\tilde{\alpha}}{\sqrt{\tilde{\gamma}}}\right]-1\right]|\tilde{f}_0^S|^4}$$

$$\times\left\{(1-i\tilde{\alpha}\sqrt{\tilde{\gamma}})\left[1-i\frac{\tilde{\alpha}}{\sqrt{\tilde{\gamma}}}\right]\ln\left[\frac{(1-i\tilde{\alpha}\sqrt{\tilde{\gamma}})\left[1-i\frac{\tilde{\alpha}}{\sqrt{\tilde{\gamma}}}\right]+|\tilde{f}_0^S|^2}{(1-i\tilde{\alpha}\sqrt{\tilde{\gamma}})\left[1-i\frac{\tilde{\alpha}}{\sqrt{\tilde{\gamma}}}\right]}\right]-\ln[1+|\tilde{f}_0^S|^2]\right\}, \tag{17a}$$

$$J(C,\tilde{\alpha},\tilde{\gamma})=\int_0^\infty \frac{d\tilde{r}\,4\tilde{r}\,e^{-2\tilde{r}^2}}{[1+|\tilde{f}_0^S|^2e^{-2\tilde{r}^2}]\left[(1-i\tilde{\alpha}\sqrt{\tilde{\gamma}})\left[1-i\frac{\tilde{\alpha}}{\sqrt{\tilde{\gamma}}}\right]+|\tilde{f}_0^S|^2e^{-2\tilde{r}^2}\right]}$$

$$=\frac{1}{\left[(1-i\tilde{\alpha}\sqrt{\tilde{\gamma}})\left[1-i\frac{\tilde{\alpha}}{\sqrt{\tilde{\gamma}}}\right]-1\right]}\frac{1}{|\tilde{f}_0^S|^2}\ln\left[\frac{(1-i\tilde{\alpha}\sqrt{\tilde{\gamma}})\left[1-i\frac{\tilde{\alpha}}{\sqrt{\tilde{\gamma}}}\right][1+|\tilde{f}_0^S|^2]}{(1-i\tilde{\alpha}\sqrt{\tilde{\gamma}})\left[1-i\frac{\tilde{\alpha}}{\sqrt{\tilde{\gamma}}}\right]+|\tilde{f}_0^S|^2}\right]. \tag{17b}$$

As in the plane-wave case, $\tilde{f}_0^{(1)}=0$. In Fig. 4 one can see the ratios $|\tilde{f}_i|/\tilde{\varepsilon}$ $(i=1,-1)$ as a function of $\tilde{\alpha}$ for $C=2$ and $\tilde{\gamma}=10^{-4}$, calculated using Eqs. (15)–(17). Comparing Fig. 4 with the analogous Fig. 5, in which are shown the values of $|f_i|/\varepsilon$ $(i=\pm1)$ calculated by Eqs. (7) and (8) of the plane-wave theory, one can observe an identical qualitative behavior; the height of the peak in Fig. 4 is reduced by a factor 1.7 with respect to the plane-wave result. Figure 6 shows the quantities $\tilde{G}_i=|\tilde{f}_i|^2/\tilde{\varepsilon}^2$ $(i=0,\pm1)$, calculated by numerical integration of Eqs. (13) for $n=0,+1,-1$ (with the adiabatic elimination of the polarization variables valid for $\gamma_\perp\gg k,\gamma_\parallel$) as a function of $\tilde{\alpha}$ and for the same values of $\gamma_\perp$, $\gamma_\parallel$, k, and C considered in the plane-wave case. There is good agreement between numerical and analytical results, except in the region around the point $\alpha=\sqrt{2}\Omega_R$.

The results show that the Rabi resonance analyzed in this paper persists in the case of a Gaussian-shaped beam. There are some quantitative differences with respect to the plane-wave case, but the qualitative picture remains unchanged.

VI. CONCLUSIONS

The previous analysis has clarified that the spectacular frequency conversion, obtained in the limit of $\tilde{\gamma}=\gamma_\parallel/\gamma_\perp\ll1$, is not so much the result of the four-wave mixing coupling, which becomes less efficient in this limit. Rather, it arises (Sec. IV) from the sluggish evolution of the phases of the two side mode fields, which becomes very slow in the limit $\tilde{\gamma}\to0$; it is well known that a slow-

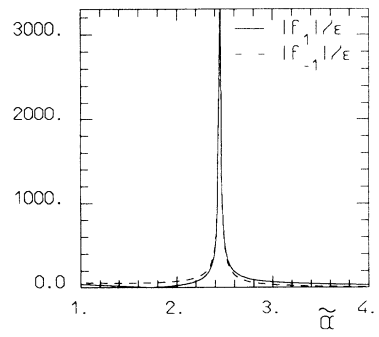

FIG. 5. Case of a plane-wave beam profile. Same as in Fig. 4, but for the plane-wave theory.

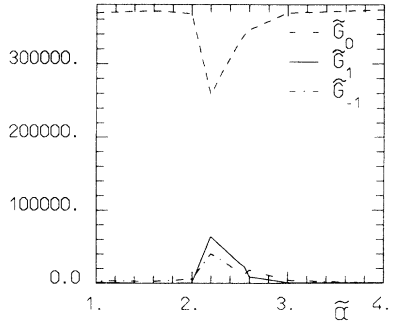

FIG. 6. Case of a Gaussian beam profile. The numerical steady-state values of $\tilde{G}_0$, $\tilde{G}_1$, and $\tilde{G}_{-1}$ as a function of $\tilde{\alpha}$, for $\gamma_\perp=10^{13}$ rad/s, $\gamma_\parallel=10^9$ rad/s, $k=3\times10^{10}$ rad/s, and $C=2$.

ing down produces an enhancement of the susceptibility of the system to external perturbation such as, for example, the injection of the weak signal.

A nice feature of the Rabi resonance in frequency conversion that we illustrate in this paper is that it is completely independent of the value of the cavity damping constant k. It represents a coherent phenomenon, completely unrelated from incoherent mechanisms such as, for example, the relaxation oscillations which are commonplace in class-B lasers and can be described by standard rate equations.

A very relevant aspect of our analysis is that it indicates the possibility of obtaining frequency conversion on the order of 100 GHz even when the relaxation rate of the population inversion (carrier density in semiconductors) is smaller than 1 GHz. As a matter of fact, since the four-wave-mixing process is mediated by the population components d_1 and d_{-1}, one would be tempted to conclude that the time scale which governs the frequency conversion is $\gamma_\parallel^{-1}$. But from our analysis it turns out that such a time scale is neither $\gamma_\parallel^{-1}$ nor that of the relaxation oscillations in class-B lasers which, when C is of order unity, scales as $(k\gamma_\parallel)^{-1/2}$. We showed that the optimum for frequency conversion is when the free spectral range α is on the order of the Rabi frequency Ω_R so that, using Eq. (10b), the frequency conversion 2α scales as $(\gamma_\perp\gamma_\parallel)^{1/2}$ when $2C$ (and hence $|f_0^S|$) has order unity. For the values of the parameters considered before as typical for semiconductor lasers ($\gamma_\parallel=10^9$ s^{-1}, $\gamma_\perp=10^{13}$ s^{-1}, $k=3\times10^{10}$ s^{-1}) one has it that the time scale $(\gamma_\perp\gamma_\parallel)^{-1/2}$ is one order of magnitude smaller than $(k\gamma_\parallel)^{-1/2}$, which in turn is one order of magnitude smaller than $\gamma_\parallel^{-1}$. Thus, our results suggest that in order to obtain frequency conversion on the order of 100 GHz it may not be necessary to exploit nonlinearities for which the response time of the carrier density is much shorter than a nanosecond, as it is done in [1].

The analysis of Sec. IV has also elucidated the deep connections which link the Rabi resonance with the multimode laser instability [3,10]. In a sense, the Rabi resonance can be considered as a precursor of the multimode laser instability, but it can be observed experimentally for values of the pump parameter substantially smaller than those required to realize the multimode laser instability. In addition, the Rabi resonance is much more robust because it persists when the laser beam has a Gaussian instead of a plane-wave configuration, whereas the multimode laser instability vanishes [13].

ACKNOWLEDGMENTS

We are grateful to Paolo Spano for suggesting this problem to us, and to Giampaolo Bava and Pierluigi Debernardi for useful discussions. This research was carried out within the framework of the Progetto Finalizzato Telecomunicazioni of the Consiglio Nazionale delle Ricerche (Research Grants No. 92.00984.PF.71 and No. 93.00804.PF.71).

[1] L. F. Tiemeijer, Appl. Phys. Lett. **59**, 499 (1991); S. Murata, A. Tomita, J. Shirnizn, and A. Suzuki, IEEE Trans. Photonics Tech. Lett. **3**, 1021 (1991); T. Mukai and T. Saito, in *Coherence, Amplification and Quantum Effects in Semiconductor Lasers,* edited by Y. Yamamoto (Wiley, New York, 1991); K. Kikuchi, M. Kakui, C. Zah, and T. Lee, IEEE Quantum Electron. **28**, 151 (1992).

[2] G. L. Mander, R. Loudon, and T. J. Shepherd, Phys. Rev. A **40**, 5753 (1989); M. Harris, R. Loudon, G. L. Mander, and J. M. Vaughan, Phys. Rev. Lett. **67**, 1743 (1991).

[3] H. Risken and K. Nummedal, J. Appl. Phys. **39**, 4662 (1968).

[4] L. A. Lugiato and L. M. Narducci, in *Fundamental Problems in Quantum Optics,* edited by J. Dalibard and J. M. Raimond (North-Holland, Amsterdam, 1992).

[5] L. A. Lugiato, in *Progress in Optics,* edited by E. Wolf (North-Holland, Amsterdam, 1984), Vol. 21, p. 69ff.

[6] N. B. Abraham, P. Mandel, and L. M. Narducci, in *Progress in Optics,* edited by E. Wolf (North-Holland, Amsterdam, 1988), Vol. 25, p. 1ff.

[7] B. R. Mollow, Phys. Rev. A **5**, 2217 (1972); F. Y. Wu, S. Ezekiel, M. Ducloy, and B. R. Mollow, Phys. Rev. Lett. **38**, 1077 (1977).

[8] See, e.g., S. Haroche and F. Hartman, Phys. Rev. A **6**, 1280 (1972).

[9] See, e.g., R. W. Boyd, M. G. Raymer, P. Narum, and D. J. Harter, Phys. Rev. A **24**, 411 (1981); S. T. Hendow and M. Sargent III, Opt. Commun. **40**, 385 (1982).

[10] R. Graham and H. Haken, Z. Phys. **213**, 420 (1968).

[11] More precisely, all the modes except $n=1$, which resonates with the signal frequency, undergo a frequency shift. This effect is, however, very small and does not affect the validity of the perturbative approach which neglects it.

[12] V. Benza and L. A. Lugiato, Z. Phys. B **35**, 383 (1979).

[13] L. A. Lugiato and M. Milani, Opt. Commun. **46**, 57 (1983).

[14] L. A. Lugiato, R. J. Horowicz, G. Strini, and L. M. Narducci, Phys. Rev. A **30**, 1366 (1984).